JOURNAL OF GEOPHYSICAL RESEARCH, VOL. 106, NO. D19, PAGES 22,707–22,724, OCTOBER 16, 2001

Constraints on the seasonal cycle of stratospheric water vapor using in situ measurements from the ER-2 and a CO photochemical clock

E. M. Weinstock,[1] E. J. Hintsa,[1,2] D. B. Kirk-Davidoff,[1] J. G. Anderson,[1] A. E. Andrews,[3,4] R. L. Herman,[5] C. R. Webster,[5] M. Loewenstein,[6] J. R. Podolske,[6] and T. P. Bui[6]

Abstract. We use in situ measurements of CO obtained in the tropics from 1995 to 1997 on the NASA ER-2 aircraft and a simple photochemical model to calculate the elapsed time between the entry of air into the stratosphere and the observation, which we define as the photochemical "age" of the air. Assuming this age represents the transit time of the air mass from a boundary at 390 K to its measured altitude, we calculate boundary condition values of CO_2 derived from in situ measurements of this species from 400 to 480 K. We validate the approach by comparing these CO_2 boundary values with an independent representation of the boundary condition from observations of CO_2 in air that had recently entered the stratosphere (as indicated by simultaneous measurements of N_2O, CO, and potential temperature). For five of the six flights, differences between CO_2 boundary condition values determined using the photochemical age of the air and those derived from independent measurements can be accounted for with isentropic mixing of midlatitude stratospheric air into the tropics. Having validated the photochemical ages of the sampled stratospheric air, we use the same analysis of in situ water data to provide water vapor boundary condition values that constrain the seasonal cycle of water vapor entering the stratosphere. On the basis of these constraints we evaluate the seasonal cycle of entry-level water vapor derived from tropical tropopause temperatures from the radiosonde network between 10°S and 10°N. We conclude that while average saturation mixing ratios provide a suitable boundary condition for water vapor entering the stratosphere, the uncertainties in saturation mixing ratios derived from radiosonde temperatures and the lack of coverage prevents distinguishing between ascent preferentially occurring over the western equatorial Pacific or throughout the tropics. With the assumption that vertical diffusion and midlatitude mixing have a negligible effect on the calculated age, ascent velocities can be inferred from the photochemical ages. These ascent velocities show a seasonal cycle that is inconsistent with our current understanding of the dynamics driving the stratospheric circulation and with independent estimates of tropical vertical ascent rates.

1. Introduction

Ever since *Brewer* [1949] proposed that transport of air from the troposphere to the stratosphere is confined to the tropics, where the cold tropopause limits stratospheric humidity, there has been ongoing research to identify and understand the processes that control the transport of air into and out of the stratosphere. Within the last 10 years, the search for the mechanism(s) controlling troposphere to stratospheric transport (STE) has gained added significance with the following: (1) observation of a possible gradual increase in stratospheric water vapor as measured by remote [*Evans et al.*, 1998; *Michelsen et al.*, 2000] and in situ [*Oltmans and Hoffman*, 1995; *Oltmans et al.*, 2000] instrumentation, and (2) understanding that increasing stratospheric water vapor concentrations decrease the threshold temperature for halogen activation in the stratosphere and potentially allow for a lengthening of the season and an expansion of the geographic region where ozone depletion occurs [e.g., *Kirk-Davidoff et al.*, 1999].

Our current understanding of the general circulation of the atmosphere has evolved from Brewer's original hypothesis to the more complex picture as discussed by *Holton et al.* [1995]. Large-scale descent at middle to high latitudes as well as diabatic ascent in the lower tropical stratosphere is under the "downward control" of eddy-induced mean zonal forces [*Haynes et al.*, 1991]. The Lagrangian mean circulation

[1] Department of Chemistry and Chemical Biology, Harvard University, Cambridge, Massachusetts, USA.
[2] Now at Woods Hole Oceanographic Institution, Woods Hole, Massachusetts, USA.
[3] Department of Earth and Planetary Sciences, Harvard University, Cambridge, Massachusetts, USA.
[4] Now at NASA Goddard Space Flight Facility, Greenbelt, Maryland, USA.
[5] Jet Propulsion Laboratory, California Institute of Technology, Pasadena, California, USA.
[6] Ames Research Center, NASA, Moffett Field, California, USA.

Paper number 2000JD000047.
0148-0227/01/2000JD000047$09.00

is supplemented by two-way isentropic transport between the tropics and the midlatitudes in the lower stratosphere. Evidence supporting the dominance of a specific mechanism controlling transport into the stratosphere is lacking. Nevertheless, the physically plausible explanation for stratospheric dehydration resulting from large-scale slow ascent with a resulting saturation mixing ratio consistent with the minimum temperature encountered is consistent with this picture of the general circulation, intriguing and most readily examined. Additionally, the link between increased atmospheric carbon dioxide and a warming of the tropical tropopause, causing a potential increase in stratospheric water vapor [*Kirk-Davidoff et al.*, 1999] provides strong impetus to carefully explore the relationship between tropical tropopause temperatures and stratospheric water vapor mixing ratios.

Initial studies comparing observed stratospheric mixing ratios to zonally averaged water vapor saturation mixing ratios derived from tropical tropopause temperatures concluded that tropical tropopause temperatures were too high to explain measured values of water vapor in the stratosphere [*Newell and Gould-Stewart*, 1981; *Danielsen*, 1982; *Russell et al.*, 1993]. This apparent disagreement could result from systematic errors in the measurement of water vapor or tropopause temperatures, from tropospheric to stratospheric transport occurring preferentially in regions of low tropopause temperatures, or some combination of these. An alternative mechanism was suggested by the in situ measurements of *Kley et al.* [1979], identifying a water vapor minimum (the hygropause) about 3 km above the local tropopause, and the series of experimental and theoretical papers that presented and analyzed the results of the Stratosphere-Troposphere Exchange Project (STEP) [e.g. *Danielsen*, 1993]: convection to altitudes significantly above the local tropopause.

Recent analyses of in situ [*Weinstock et al.*, 1995] and satellite [*Mote et al.*, 1995, 1996; *Abbas et al.*, 1996] tropical stratospheric water vapor data along with correlations of carbon dioxide and water vapor in the midlatitude stratosphere [*Boering et al.*, 1995] have shown that the hygropause observed a few kilometers above the tropopause during Northern Hemisphere (NH) summer is consistent with the vertical propagation of a water vapor minimum from the previous winter. While it has long been known that tropical tropopause temperatures exhibit a seasonal cycle [*Reed and Vleck*, 1969; *Reid and Gage*, 1981], it is only the recent analysis of the Halogen Occultation Experiment (HALOE) tropical water vapor data which has illustrated the correlation of water vapor mixing ratios at the tropopause with the seasonal cycle of tropical tropopause temperatures [*Mote et al.*, 1995, 1996]. *Jackson et al.* [1998] used HALOE water vapor data in the tropopause region to explore where cross-tropopause transport occurs, as well as what regions appeared to be dehydrated based on The National Centers for Environmental Prediction (NCEP) reanalysis data. From an analysis of the water vapor fields in the tropopause region, Jackson et al. suggest that most of the dry air enters the stratosphere between the equator and 10°N in the December to February timeframe, with sporadic transport of dry air occurring from March to August. They also see evidence of wetter air transported into the stratosphere from September to November from 10°S to 20°N at longitudes close to 120°E.

In contrast to earlier studies, *Dessler* [1998] demonstrated that zonally and annually averaged saturation mixing ratios derived from tropical tropopause temperatures are not inconsistent with determinations of the annual average water vapor mixing ratio entering the stratosphere, $(H_2O)_e$. However, because of limitations in the spatial coverage of the radiosonde network, and the spread in measured $(H_2O)_e$, Dessler's analysis did not rule out the possibility that most of the cross-tropopause transport, in any or all seasons, occurs in the western tropical Pacific, the so-called "stratospheric fountain" region [*Newell and Gould-Stewart*, 1981], as discussed below. Additionally, a recent climatological analysis of tropical tropopause temperatures [*Seidel et al.*, 2001] demonstrated a gradual decrease in annual average tropical tropopause temperatures during the past three decades, equivalent to an average decrease in water vapor saturation mixing ratio of about 0.3 ppmv per decade. This trend suggests that the average water vapor mixing ratio entering the stratosphere two decades ago was about 0.6 ppmv less than that reported by *Dessler*[1998] and thus tends to support the assertion by *Voemel and Oltmans* [1999] that the need to invoke a stratospheric fountain hypothesis to explain the dryness of the stratosphere two decades ago is not, in fact, ruled out by Dessler's analysis. However, a decrease in annual average tropical tropopause temperatures is not consistent with either the recent observed increases in stratospheric water vapor or the analysis of *Hurst et al.* [1999], indicating no observable trend in stratospheric water vapor from 1993 to 1997. Furthermore, arguments for the importance of convection on the stratospheric water vapor budget have recently been published [*Sherwood and Dessler*, 2000, 2001], thereby helping to maintain the level of uncertainty of this critical issue.

A primary goal of this paper is to develop an approach suitable for testing proposed mechanisms for troposphere to stratosphere transport by using in situ measurements to determine the seasonal cycle of water vapor entering the stratosphere. This requires either the direct measurement of water vapor mixing ratios where air enters the stratosphere, $(H_2O)_{bc}$ (most often thought of as the tropical tropopause), or measurements within the stratosphere, $(H_2O)_m$, with the development of a method to convert $(H_2O)_m$ to $(H_2O)_{bc}$. We will call this calculated water vapor stratospheric boundary condition $(H_2O)_{mbc}$. As water vapor, carbon dioxide exhibits a seasonal cycle in the stratosphere. However, unlike water vapor, the CO_2 seasonal cycle originates at the surface and results from the uptake and release of CO_2 from the biosphere. At the surface the amplitude and phase of the seasonal cycle vary with latitude with the largest amplitudes observed in the NH [*Conway et al.*, 1994]. This seasonal cycle is superimposed on the long-term increase caused by fossil fuel combustion. Both the seasonal cycle and the long-term increase have been observed to propagate into the stratosphere [*Boering et al.*, 1994, 1995, 1996]. Because the variability in CO_2 mixing ratios is imposed mainly by sources and sinks at the surface, CO_2 mixing ratios in the vicinity of the tropical tropopause are relatively homogeneous. Accordingly, $(CO_2)_{bc}$ can be directly determined from measurements near the tropical tropopause [*Boering et al.*, 1994; *Andrews et al.*, 1999]. In contrast, direct measurement of $(H_2O)_{bc}$ is made implausible by the significant thermal, spatial, and temporal variability at the tropical tropopause, where the stratospheric water vapor boundary condition is set.

The approach used here to derive $(H_2O)_{mbc}$ from in situ measurements in the lower stratosphere uses a simple photochemical model constrained by measured CO and an

empirical relationship between OH and solar zenith angle to calculate the elapsed time between the date an air mass crossed the 390 K isentrope and the date it was sampled. We validate this framework by using the photochemical age to construct a time series of entry-level CO_2 mixing ratios, hereinafter called $(CO_2)_{mbc}$, and compare that with a stratospheric boundary condition derived from in situ measurements of CO_2 in air that had recently entered the stratosphere, as indicated by simultaneous measurements of N_2O, CO, and potential temperature, hereinafter called $(CO_2)_{bc}$ [*Andrews et al.*, 1999]. The in situ data for H_2O, CO, and CO_2 were acquired during the Stratospheric Tracers of Atmospheric Transport (STRAT) mission from May 1995 to December 1996 and the Photochemistry of Ozone Loss in the Arctic Region in Summer (POLARIS) mission from April to September 1997 using the NASA ER-2 aircraft.

We then quantitatively compare boundary condition water vapor mixing ratios derived from this method, with saturation mixing ratios using tropical tropopause temperatures from radiosonde data taken between 10°S and 10°N used as an independent representation of $(H_2O)_{bc}$. While the primary mechanism for dehydration in the tropopause region has not been identified, we compare measured water vapor mixing ratios with saturation mixing ratios derived from the cold-point tropopause as opposed to the standard WMO tropopause because this minimum temperature can most easily be associated with a simple physical process leading to dehydration as air is ascending into the stratosphere. The criteria for the radiosonde stations chosen for this comparison are similar to those used by *Dessler* [1998]. Additionally, we investigate any bias in the derived average saturation mixing ratios that might result from the geographic distribution of stations, heavily weighted to the western tropical Pacific region.

If transport in the lower tropical stratosphere is consistent with the "tropical pipe" model [*Plumb*, 1996], with purely advective ascent, and there were no sources or sinks for H_2O and CO_2, our method would provide a time series of entry-level mixing ratios for these species that would exactly represent the average stratospheric boundary condition. However, the oxidation of methane is a source of both water vapor and CO_2 in the stratosphere. Also, studies have indicated that air sampled in the lower tropical stratosphere is made up of up to 50% air isentropically mixed in from midlatitudes [*Minschwaner et al.*, 1996; *Volk et al.*, 1996; *Flocke et al.*, 1999]. Accordingly, the "leaky pipe" model developed by *Neu and Plumb* [1999] which includes isentropic mixing from midlatitudes better describes the processes that control the composition of air parcels in the lower tropical stratosphere. Consistent with experimental evidence and the "leaky pipe" model, we explore how well isentropic mixing improves the agreement between $(CO_2)_{mbc}$ and $(CO_2)_{bc}$ and then use the mixing scenario that gives the best match between the two to provide water vapor boundary condition values, $(H_2O)_{mbc}$.

2. Experimental Description

All the data presented here were taken on the NASA ER-2 during the STRAT and POLARIS missions in different seasons from May 1995 to September 1997. Tropical profile data were obtained during excursions from cruise altitudes of about 20 km down to 15 km and back (hereinafter referred to as dives) near the southernmost extent of southbound survey flights from Barbers Point, HI (22°N). These tropical dives took place on 951105 (dates in YYMMDD format), 960213, 960801, 960808, 961211, and 970923. The data presented here are from the dive regions between 2°S and 10°N, with some of the northernmost data points removed (specifically from the 960213 flight), because the measured ratio of NO_y to O_3 for these points is characteristic of midlatitude air [*Murphy et al.*, 1993].

A detailed description of the fast-response Lyman-α photofragment hygrometer has been given previously [*Weinstock et al.*, 1994]. On the basis of extensive laboratory calibrations and comparison with in-flight absorption measurements in the upper troposphere its accuracy is ±5% [*Hintsa et al.*, 1999]. Carbon dioxide is measured by nondispersive infrared absorption with an uncertainty < 0.1 ppmv; data are reported relative to the Scripps Institution of Oceanography/World Meteorological Organization 1995 mole fraction scale, which has an accuracy of ±0.1 ppmv [*Boering et al.*, 1994]. CO and CH_4 are measured by the Aircraft Laser Infrared Absorption Spectrometer (ALIAS) [*Webster et al.*, 1994; *Herman et al.*, 1999] with an estimated accuracy of 5%. N_2O is measured by the Airborne Tunable Laser Absorption Spectrometer (ATLAS) [*Podolske and Loewenstein*, 1993] with an estimated uncertainty of 3.5% [*Strahan*, 1999]. Static temperature and pressure are measured by the Meteorological Measurement System [*Scott et al.*, 1990].

Plates 1a and 1b present the carbon dioxide and water vapor data, respectively, for the tropical dives, plotted as a function of potential temperature θ. The differences between profiles result from the seasonal cycle and annual increase of carbon dioxide [e.g., *Boering et al.*, 1996] and the seasonal cycle of water vapor [*Weinstock et al.*, 1995; *Mote et al.*, 1996] in air at the tropical tropopause, followed by any dynamical and/or photochemical processes that affect these values as the air ascends. Methane oxidation in the stratosphere produces both carbon dioxide and water vapor. This production is easily accounted for when simultaneous observations of methane are available. For flights in which high-resolution methane is not available, methane mixing ratios are determined from a fit to N_2O data determined from other tropical flight data. The contribution to CO_2 in the lower tropical stratosphere is < 0.1 ppmv and is neglected in this analysis.

3. Analysis

Tropical profiles of CO versus potential temperature for the flights discussed here are shown in Figure 1. These profiles are remarkably similar, suggesting the possibility of using a single average profile to determine average ascent velocities for the analysis of all the flights [e.g., *Flocke et al.*, 1999]. We choose nevertheless to analyze each flight separately, allowing for a seasonal variation in ascent velocity. The lifetime of CO is 3-4 months just above 390 K, where it has a mixing ratio of about 42 ppbv. The CO mixing ratio plotted in Figure 1 decays with increasing altitude, approaching a steady state value of about 12 ppbv near 480 K. The change in the concentration of CO in the stratosphere is determined by a balance between loss through reaction with OH,

(R1) $CO + OH + O_2 \rightarrow \rightarrow CO_2 + HO_2$,

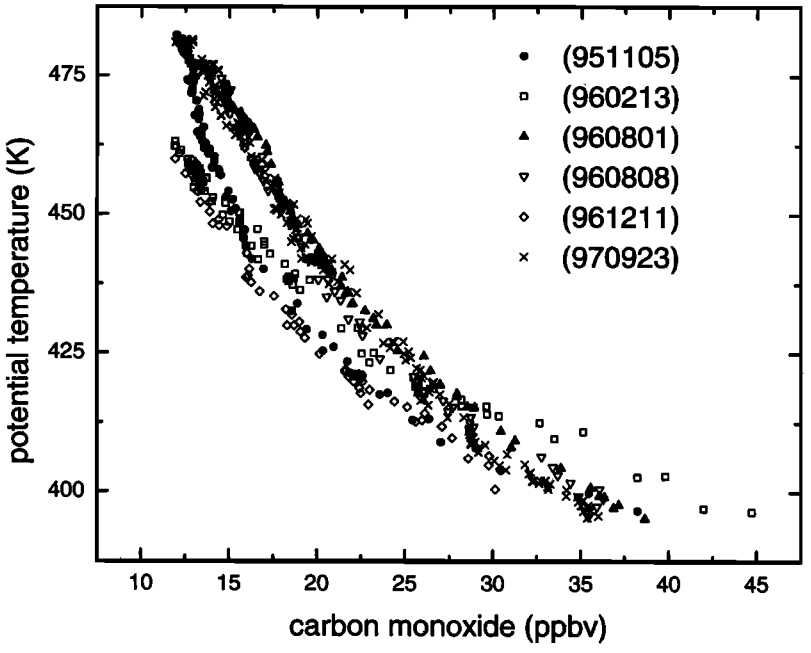

Figure 1. Mixing ratio profiles of CO versus potential temperature for the six tropical dives during the STRAT and POLARIS missions.

and production from the reaction of OH with CH_4,

(R2) $OH + CH_4 \rightarrow \rightarrow CO$ + products,

where the series of reactions that lead to CO production, summarized by (R2), have been presented, for example, by *Le Texier et al.* [1988]. We assume that CO production from CH_4 and $O(^1D)$ are negligible in the lower tropical stratosphere. From these two reactions the change in CO concentration as a function of time can be expressed as

$$\frac{d[CO]}{dt} = k_2[CH_4][OH] - k_1[CO][OH]. \quad (3)$$

Integrating equation (3) to solve for elapsed time in the stratosphere, we obtain

$$\int_{[CO]_0}^{[CO]_m} d[CO] = \int_{t_0}^{t_m} (k_2[CH_4][OH] - k_1[CO][OH])dt \quad (4)$$

where t_0 is the date the air mass crossed the 390 K isentrope (about 17 km) and entered the stratosphere, with [CO] = $[CO]_0$, and t_m is the date the air mass was encountered, with [CO] = $[CO]_m$. We define the elapsed time in the stratosphere, $t_m - t_0$, as the photochemical age of the air mass. We choose 390 K to represent the lower boundary of the stratospheric overworld because it is the lowest isentrope above which vertical transport is almost entirely controlled by diabatic ascent. Below 390 K, vertical mixing can be important because the tropopause height exhibits significant variability associated with wave activity, cloud height, or other meteorological conditions. This choice has implications for the analysis of both carbon dioxide and water vapor. *Boering et al.* [1994] found a 2-month lag between surface measurements and those at 390 K in the tropics consistent with the seasonal cycle of carbon dioxide originating in the boundary layer. For this analysis we assume the water vapor mixing ratio is set at the average cold-point tropopause (376 ± 5 K). We estimate an ascent time between that isentrope and 390 K of about 20 days on the basis of profiles of CO and CO_2 in this region.

To find t for each datum in each dive, equation (4) is integrated iteratively using a timestep of 1 hour, varying t_0 until $[CO]_m$ is within 2% of the observed [CO]. To do this, we need to know how each of the variables changes as a function of that time. Both k_1 and k_2 [*DeMore et al.*, 1997] will exhibit a time dependence, because k_1 is pressure dependent and k_2 is temperature dependent. Accordingly, solving equation (3) for t requires knowledge of both T and P as a function of elapsed time since the air mass entered the stratosphere. Profiles of T and P plotted versus potential temperature for the tropical dives exhibit a variability of approximately ±5 K and 5 mbar, respectively, in the lower tropical stratosphere. We use these profiles to obtain an average fit of pressure and temperature to potential temperature. For each calculation of the CO mixing ratio, we start with an assumed ascent rate to obtain the relationship between elapsed time and potential temperature. We then use these fits to provide temperature and pressure as a function of time in the stratosphere. We use a value of $[CO]_0$ of 42 ppbv (the approximate average of the tropical dives; variability is ±5 ppbv) for all the dives. Typically, values of CH_4 in the lower tropical stratosphere range from 1.6 to 1.7 ppmv. In the calculation we approximate the CH_4 mixing ratio as 1.7 ppmv, resulting in a small uncertainty in the (relatively small) rate of production of CO. Even though we assume a constant mixing ratio for CH_4, its concentration depends on density, and therefore elapsed time in the stratosphere. Because OH correlates with solar zenith angle (SZA), it also exhibits a slight dependence on time in the stratosphere, because even in the tropics, SZA varies with the day of the year. The diurnal cycle of OH used in the model is determined from a fit of measured OH in the stratosphere [*Wennberg et al.*, 1995, 1998] to solar zenith angle. We show in Plate 2 OH concentrations plotted as a function of SZA for

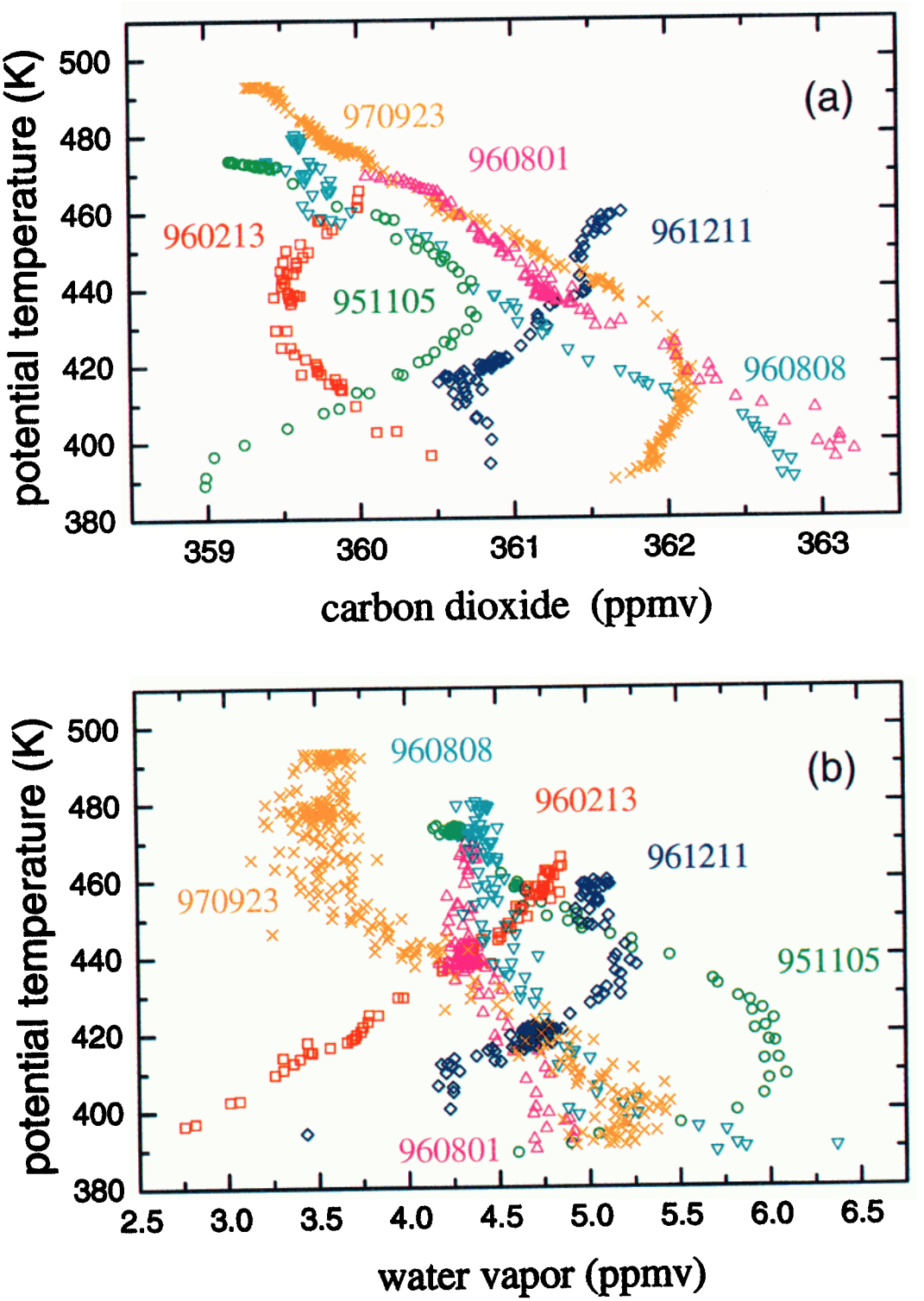

Plate 1. Mixing ratio profiles versus potential temperature for the six tropical dives during the STRAT and POLARIS missions: (a) carbon dioxide and (b) water vapor.

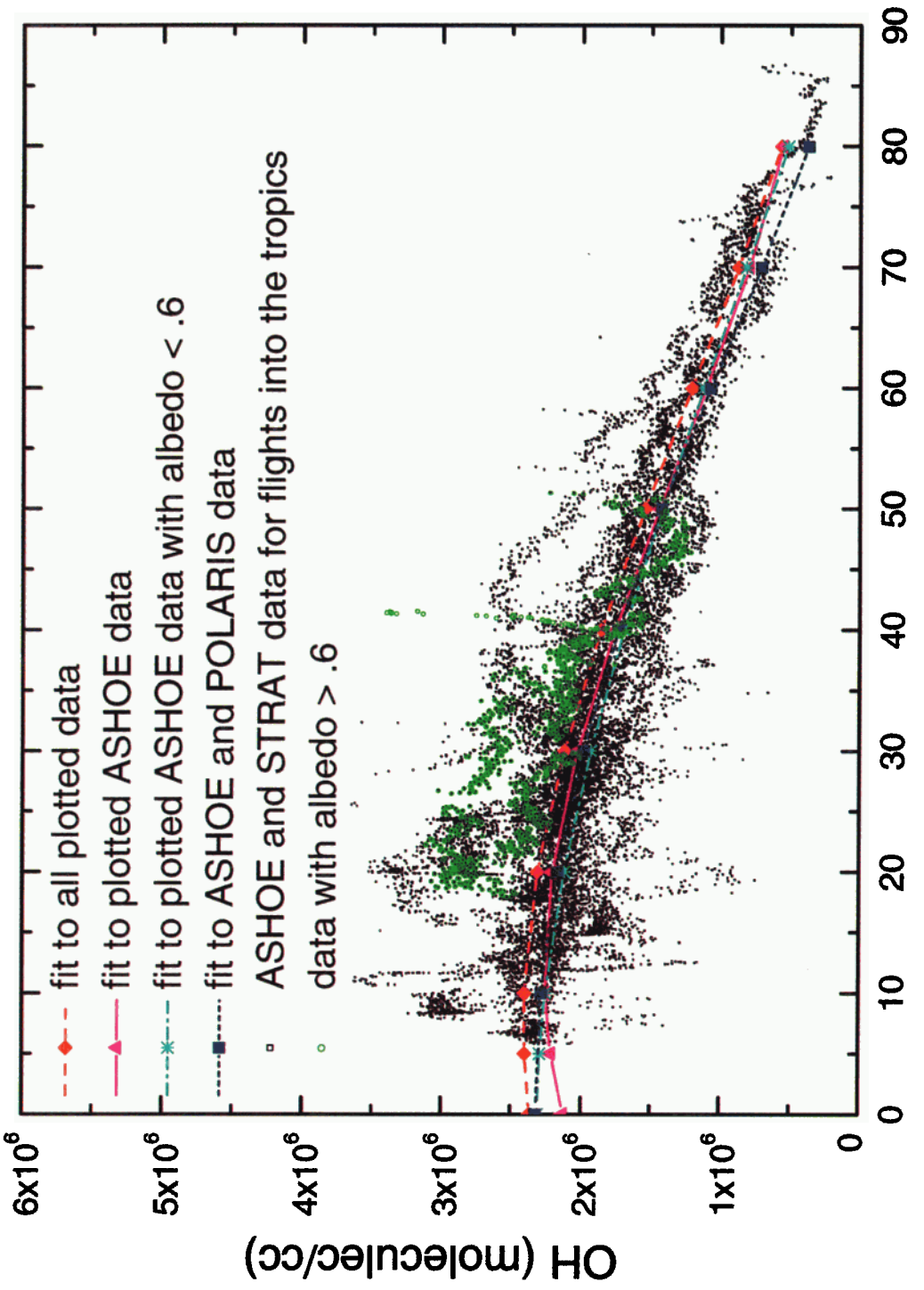

Plate 2. OH concentrations plotted as a function of solar zenith angle for data taken within 22° latitude of the equator for flights into the tropics during the ASHOE and STRAT campaigns. Data from those flights with albedo > 0.6 are plotted separately. Also shown are polynomial fits to all the data plotted, fits to subsets of the data as described in the legend, and a fit to all OH data from the ASHOE and POLARIS campaigns.

data taken within 22° latitude of the equator for flights into the tropics, as well as data selected during the flights with significant cloud cover, resulting in an albedo > 0.6, thereby increasing production. We also include fits to all the data, as well as to subsets of the data as described in the legend, and a fit to all Airborne Southern Hemisphere Ozone Experiment (ASHOE) and POLARIS data. This plot shows less than 10% variation in the different fits of OH to solar zenith angle, but it also illustrates the potential for underestimating OH under conditions of high albedo. However, zonal transport, with an approximately 3-week transit around the globe, averages out the effects of longitudinal variations in albedo.

4. Results and Discussion

Plots of photochemical age versus θ are shown in Figure 2a. Figure 2b shows the calculated date that the air mass crossed the 390 K isentrope plotted versus θ. These dates are obtained by subtracting the photochemical age from the flight date for each air mass. On 961211 the region between 405 and 425 K was characterized by low N_2O values, indicative of air that had recently been transported from higher latitudes. This midlatitude character might be responsible for some of the structure in the photochemical age for that flight. However, in other cases, photochemical ages were insensitive to variability in N_2O values and thus, presumably, to mixing with air from higher latitudes. N_2O values were considerably lower on 960808 than on 960801, but the corresponding photochemical ages are nearly identical.

Figure 3 presents CO_2 and H_2O mixing ratios (corrected for methane oxidation) from the six STRAT and POLARIS flights plotted against the date that the air mass represented by each data point crossed the 390 K isentrope, $(CO_2)_{mbc}$ and $(H_2O)_{mbc}$, respectively. The solid curve plotted in Figure 3a represents the stratospheric boundary condition for CO_2 that was derived from observed CO_2 mixing ratios during 17 ER-2 deployments from 1992 to 1997 [*Andrews et al.*, 1999].

In Figure 3b the solid curve shows a time series of average minimum saturation water vapor mixing ratio (WVSMR) calculated using radiosonde data archived at NASA Goddard Space Flight Center from soundings between 10°S and 10°N. For each sounding, of which the minimum pressure was less than 90 mbar, the minimum WVSMR was found. All such minima less than 20 ppmv were retained, and the rest were discarded, following *Dessler* [1998]. The solid curves were calculated by averaging over all soundings for a given day and subjected to a 30-day running mean. There is a ±10% uncertainty for these saturation mixing ratios derived from an estimated ±0.5-1 K uncertainty in the measured temperatures [*Luers and Eskridge*, 1998].

The level of agreement in both phase and magnitude between values of $(H_2O)_{mbc}$ and $(H_2O)_{bc}$ exhibited in Figure 3b is comparable to that between $(CO_2)_{bc}$ and values of $(CO_2)_{mbc}$ plotted in Figure 3a for the corresponding flights. NH summer water vapor boundary condition mixing ratios derived from observations on the ER-2 and the model appear to be consistent with tropopause saturation mixing ratios for both 1995 and 1996. However, the 961211 CO_2 data show significant attenuation from $(CO_2)_{bc}$, suggesting that the water vapor agreement for the summer of 1996 inferred from the 961211 data is fortuitous. The data points above 5.3 ppmv water vapor from the 960808 flight and the data points below 3 ppmv for 960213 correspond to air sampled near or below the 400 K isentrope. On the basis of water vapor measurements taken during the Central Equatorial Experiment (CEPEX) [*Weinstock et al.*, 1995], air in this region has not

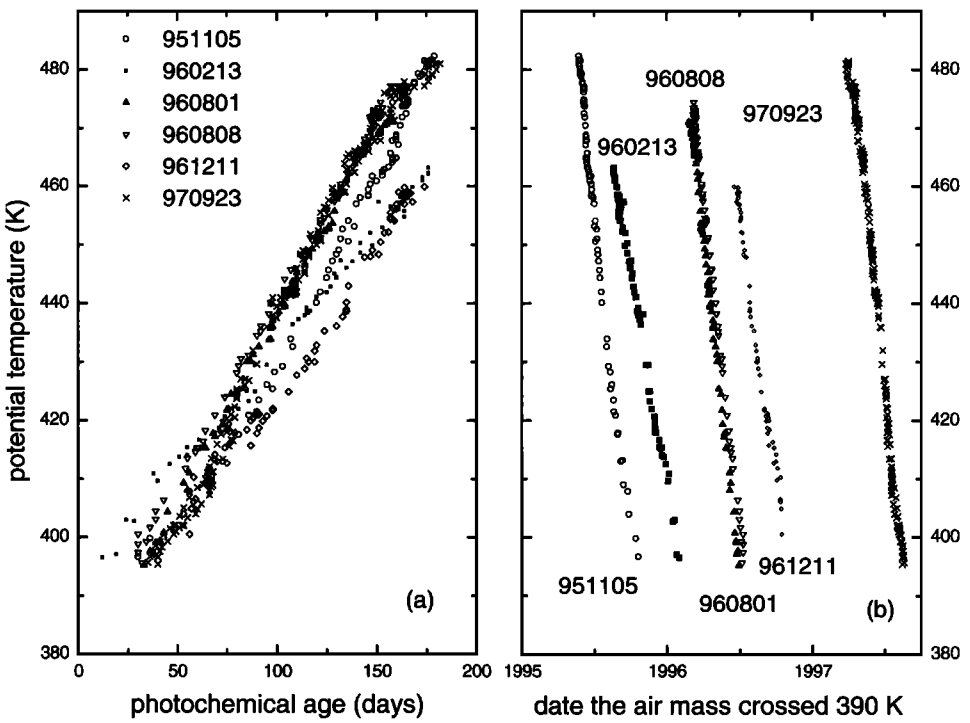

Figure 2. Plots of (a) days since the air mass crossed the 390 K isentrope, or photochemical age, and (b) date the sampled air mass crossed the 390 K isentrope, versus potential temperature for the six tropical profiles.

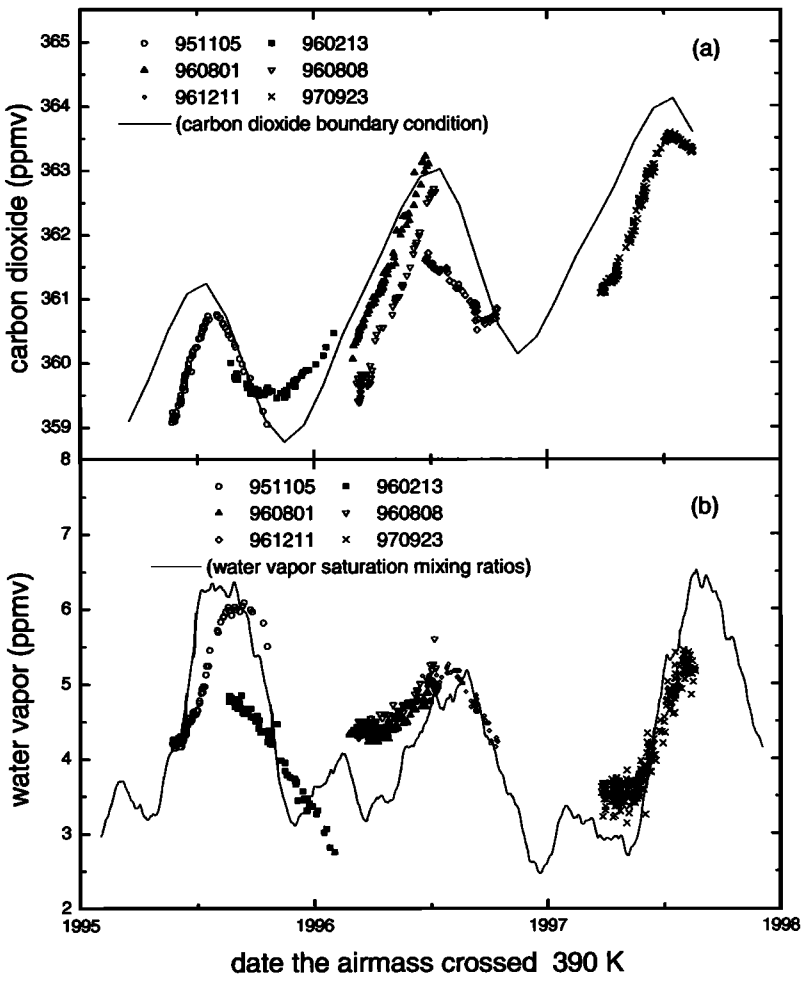

Figure 3. Mixing ratios measured above the tropopause plotted versus the date that the sampled air mass crossed the 390 K isentrope as determined by measured CO and the photochemical model: (a) carbon dioxide and (b) water vapor. Included in Figure 3a is a plot of $(CO_2)_{bc}$, boundary condition values determined from tropopause measurements as described in the text. Included in Figure 3b is a plot of running mean WVSMRs derived from cold-point temperatures from radiosonde data between 10°S and 10°N.

yet undergone zonal mixing; its water vapor mixing ratio is still consistent with the local tropopause temperature it experienced and, accordingly, cannot be expected to match average boundary condition values.

Above 400 K the clearest differences exhibited between the boundary condition values derived from the model and those derived from tropopause measurements are exhibited by the oldest air in the profiles, as expected. For example, as shown in Figure 3, air sampled near the 430 K isentrope in the 951105 profile and the oldest air in the 960213 profile crossed the 390 K isentrope during approximately the same days of the year. However, during the three months between the two flights, both the water vapor and the carbon dioxide mixing ratios in these air masses were significantly altered by diffusive processes. Accordingly, the fact that agreement exhibited in Figure 3b between $(H_2O)_{mbc}$ and $(H_2O)_{bc}$ is comparable to that between $(CO_2)_{mbc}$ and $(CO_2)_{bc}$ exhibited in Figure 3a does not sufficiently constrain $(H_2O)_{bc}$. We therefore must explore the diffusive processes responsible for the disagreement exhibited by CO_2 in order to investigate the sensitivity of $(H_2O)_{mbc}$ to these processes.

5. Mixing From Midlatitudes

Several recent studies have shown that on average, 30-50% of the air in the lower tropical stratosphere has been transported isentropically from midlatitudes [*Avallone and Prather*, 1996; *Volk et al.*, 1996; *Minschwaner et al.*, 1996; *Herman et al.*, 1998; *Flocke et al.*, 1999]. We now consider how well such mixing of midlatitude air into the tropics can account for the differences between $(CO_2)_{mbc}$ and $(CO_2)_{bc}$. It is important to emphasize that we are primarily trying to investigate only whether the mixing in of midlatitude air, as constrained by profiles observed in the tropics and midlatitudes, can account for the differences observed in Figure 3a. Ultimately, the goal is to find a plausible mixing scenario that yields $(CO_2)_{mbc}$ which matches $(CO_2)_{bc}$ well enough that the resulting $(H_2O)_{mbc}$ can be used to constrain $(H_2O)_{bc}$.

However we account for mixing in the model, we must first determine the dependence of water vapor and CO_2 on potential temperature and day of the year in midlatitudes. In the tropics there is a compact relationship between potential

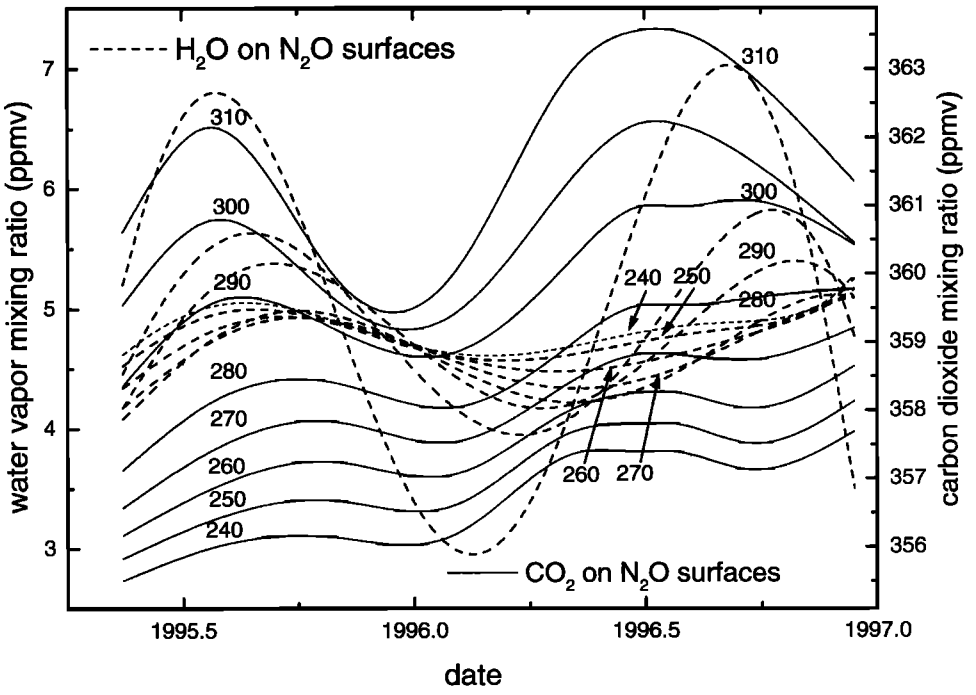

Figure 4. CO_2 and water vapor on N_2O surfaces (310 ppbv to 240 ppbv) plotted as a function of date that the measurement took place. The lines are polynomial fits to the measured data points. The N_2O surfaces are labeled in parts per billion by volume (ppbv), with the labels on the left-hand side corresponding to plots of CO_2 on N_2O surfaces and those on the right-hand side to plots of H_2O. The data points are taken from fits to plots of water vapor and CO_2 versus N_2O from the 950515, 951031, 960202, 960725, 960921, and 961213 flights during the STRAT mission, between 30° and 41°N. To aid in the seasonal polynomial fits, some additional data points are added to the 1995 calendar year data from the following year. The water vapor data points for day number -101 (day number 264 of calendar year 1995) are from the data taken on day number 264 (of calendar year 1996). The carbon dioxide and water vapor data points for day number -157 as well as the carbon dioxide data points for day number 178 (arbitrarily chosen to help constrain the polynomial fit) are from data taken on day number 208. For day number -157, carbon dioxide is reduced by 1.4 ppmv to approximately account for its annual growth rate.

temperature and CO_2 or H_2O mixing ratios. In midlatitudes, however, mixing from planetary waves causes significant variability along an isentrope [e.g., *Boering et al.*, 1996, Figure 1]. However, compact relationships do exist between N_2O, CO_2, and H_2O at midlatitudes [e.g., *Hintsa et al.*, 1994; *Boering et al.*, 1995]. Plots of CO_2 and water vapor on N_2O surfaces are presented in Figure 4 as a function of observation date. The curves are polynomial fits to the data. The plots in Figure 4 illustrate that the CO_2 seasonal cycle that originates in the tropics is maintained in the midlatitude lower stratosphere, consistent with the results of *Boering et al.* [1994] and *Andrews et al.* [1999]. This seasonal signature would not be exhibited as clearly if CO_2 and water vapor were binned by potential temperature because of reversible displacements of tracer isopleths associated with planetary scale waves. Water vapor data on the 310, 300, and 290 N_2O isopleths plotted in Figure 4 do not fit the curves nearly so well as the corresponding CO_2 data, possibly because the water vapor mixing ratios in the younger air transported to midlatitudes do not represent an average of water vapor mixing ratios of air entering the stratosphere in the tropics. Nevertheless, the phase relationship between the seasonal cycles of water vapor and CO_2 exhibited in the tropical and midlatitude lower stratosphere could potentially elucidate details of the mixing process.

To determine $(CO_2)_{mbc}$ and $(H_2O)_{mbc}$ we start with the air parcel observed in the lower tropical stratosphere, which contains both tropical and midlatitude components. We reverse the actual physical process or, in the terminology of *Mote et al.* [1995], rewind the tape recorder and "remove" the midlatitude components as the "descending" air reaches the specified isentropes, leaving behind the purely tropical component that we compare to $(CO_2)_{bc}$ and $(H_2O)_{bc}$ in Figures 5 and 7. For example, for CO_2 this process can be represented by the following equations:

$$(CO_2)_{measured}=(CO_2)_{mbc}*(1-fr_{ml})+(CO_2)_{ml}*fr_{ml}, \quad (5)$$

which when solved for $(CO_2)_{mbc}$ gives

$$(CO_2)_{mbc}=[(CO_2)_{measured}-(CO_2)_{ml}*fr_{ml}]/[1-fr_{ml}], \quad (6)$$

where fr_{ml} is the fraction of midlatitude air mixed in on a prescribed isentrope, $(CO_2)_{ml}$ is the CO_2 mixing ratio of the midlatitude air mass, $(CO_2)_{measured}$ is the CO_2 mixing ratio measured in the tropics, and $(CO_2)_{mbc}$ is as previously defined. When simulating midlatitude mixing, the data are binned at 5° potential temperature intervals. The N_2O values [*Podolske*

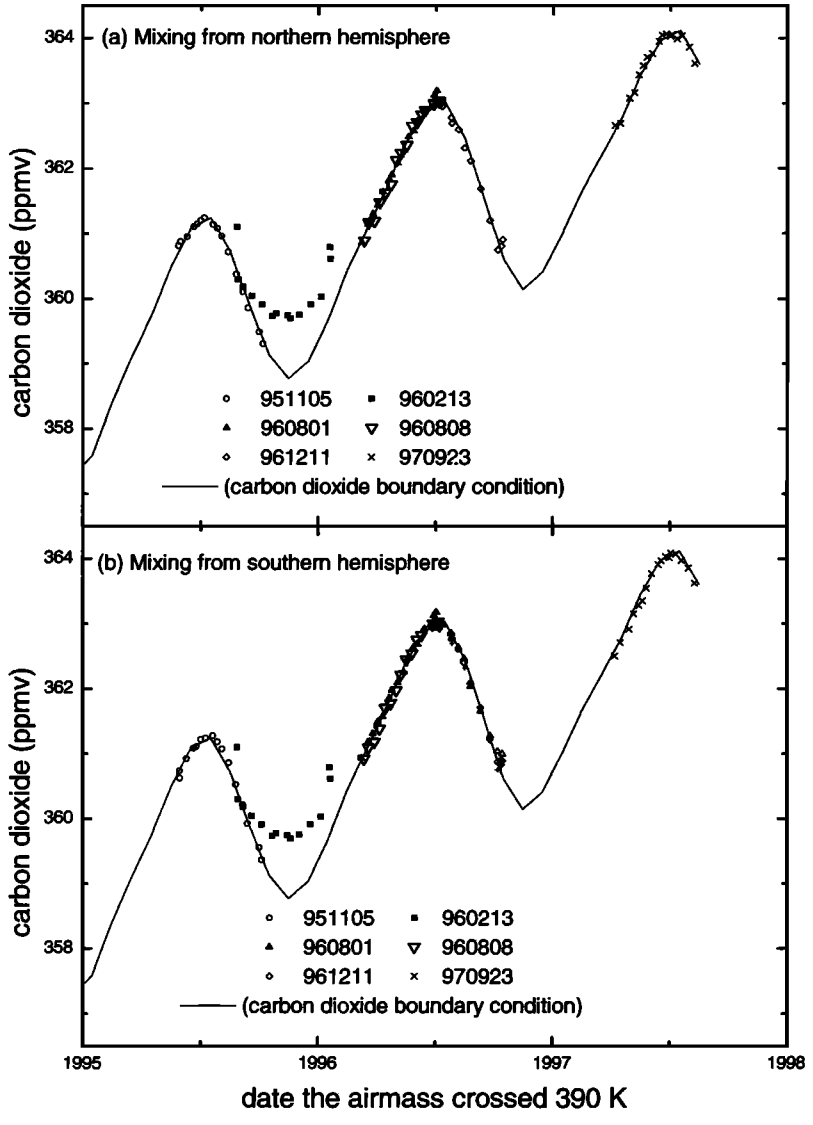

Figure 5. Mixing ratios of carbon dioxide for the 951105, 960213, 960801, 960808, 961211, and 970923 flights derived from measured mixing ratios by removing prescribed fractions of midlatitude air as described in the text, plotted versus the date the sampled air mass crossed the 390 K isentrope as determined by measured CO and the photochemical model. Included in the plot is $(CO_2)_{bc}$. Figures 5a and 5b result from using Northern and Southern Hemisphere air, respectively.

and Loewenstein, 1993] used to derive the midlatitude CO_2 and H_2O mixing ratios correspond to the average N_2O mixing ratios on these isentropes at northern midlatitudes. Because there are no Southern Hemisphere (SH) midlatitude measurements of N_2O, H_2O, and CO_2 for the 1995-1997 time period, we assume that SH midlatitude tracer-tracer correlations are identical to those in the NH midlatitudes. The relation between midlatitude N_2O and potential temperature is based on seasonal climatologies [*Strahan et al.*, 1999] for the Northern and Southern Hemispheres. It is worth noting, however, that Strahan's climatology for the SH is based only on measurements taken during 1994.

While in situ N_2O profiles in the lower tropical stratosphere exhibit mixing ratios indicative of midlatitude mixing [*Volk et al.*, 1996; *Minschwaner et al.*, 1996, *Herman et al.*, 1998], the long lifetime of N_2O precludes it from being a good indicator of young midlatitude air. Also, in situ data show evidence of significant variability in N_2O-θ correlations within a season. Accordingly, we do not use measured N_2O to constrain the amount of mixing, but we do derive for each mixing scenario N_2O mixing ratios equivalent to the purely tropical component, $(N_2O)_{tr}$, to evaluate the extent to which the amount of mixing that provides the best fit of $(CO_2)_{mbc}$ to $(CO_2)_{bc}$ yields a reasonable value of $(N_2O)_{tr}$.

We do not take into account the CO content of the admixed air in the photochemical age calculation. However, we can estimate the maximum error in CO caused by the neglect of mixing. With 20% mixing of midlatitude air containing half as much CO as in the tropical profile on the 410 K isentrope (the worst case based on comparing tropical and midlatitude STRAT profiles), measured CO would be 10% lower than in pure tropical air, with a resulting calculated photochemical age for this one point about 30% too high. However, the impact of even such a severe mixing event on calculated

Table 1. Range of the Fraction of Midlatitude Northern and Southern Hemisphere Air Mixed Into the Tropics Needed to Convert CO_2 Measured in the Lower Tropical Stratosphere to $(CO_2)_{bc}$ for Five of the Tropical Flight Profiles[a]

Flight Date	951105	960801	960808	961211	970923
Mixing fraction from NH	0.22-0.38	0.02-0.42	0.16-0.84	0.15-0.68	0.40-0.63
Mixing fraction from SH	0.10-0.19	0.01-0.37	0.10-0.53	0.02-0.41	0.12-0.40

[a] Range of air shown corresponds to all the midlatitude air mixed into the youngest and oldest air masses encountered in each flight since they entered the stratosphere.

ascent times for air parcels sampled above 430 K is less than 10%. For most mixing events, midlatitude CO is only 10 to 25% below tropical values [*Herman et al.*, 1999], and the impact on photochemical age would be much less.

Figures 5a and 5b illustrate how well for five of the six flights this mixing approach, using Southern and Northern Hemisphere air, respectively, provides values for $(CO_2)_{mbc}$ that match $(CO_2)_{bc}$. For all the profiles, the N_2O-θ correlations were derived from *Strahan*'s climatology [1999] for each hemisphere, which is normalized to 1997 values of N_2O. We do not correct the 1995 and 1996 N_2O climatology data for the 0.2%/y growth rate of N_2O, but this has a negligible effect on the analysis. The best fit between $(CO_2)_{mbc}$ and $(CO_2)_{bc}$ was determined by varying the values of fr_{ml} to minimize $q=\mathrm{sqrt}\{\Sigma[(CO_2)_{bc} - (CO_2)_{mbc}]^2\}$. We list in Table 1 the ranges of the fraction of air used to mix in for each flight. These fractions represent the sum of the individual fr_{ml} mixed in on each isentrope for each data point. In general, there is a direct correlation in each flight between the time the air is in the stratosphere and the fraction of midlatitude air mixed in. Additionally, somewhat more mixing is typically required when using NH air. The fact that for some flights the mixing scenario utilizes a mixing fraction of greater than 60% NH air, which is more than previous studies have typically shown, might be an indication that the mixing is predominantly from the SH.

Because we are ultimately interested in the sensitivity of the derived $(H_2O)_{mbc}$ to different mixing scenarios, modeling the mixing from the Southern and Northern Hemispheres independently gives an indication of this sensitivity. However, limited data results in more uncertainty in the mixing ratios of CO_2 and H_2O mixed in on a given isentrope from the SH. Accordingly, the ultimate purpose of using mixing from the SH is to support the results obtained using NH midlatitude air in the mixing. Except for the 960213 flight, for which the mixing model does not provide a reasonable match of $(CO_2)_{mbc}$ with $(CO_2)_{bc}$, a small value of $q \leq 0.3$ is typically obtained. For the 960213 flight, mixing ratios of N_2O and fluorocarbons indicate a large filament of midlatitude air was encountered between the 405 and the 425 K isentropes. The very low water vapor data below the 405 isentrope represents air that has retained the temperature signature of a cold tropopause region.

Figures 6a and 6b illustrate that the corresponding N_2O profiles, which emerge from the mixing process, are reasonably consistent with hypothetical N_2O profiles of purely tropical air, unperturbed by midlatitude mixing, designated here as $(N_2O)_{tr}$. The profile of $(N_2O)_{tr}$ was produced by taking a tropospheric value of 315 ppbv which decays through photolysis during ascent in the stratosphere, using an average lifetime of 63 years and an average ascent rate of 0.53 K/d. In general, the Strahan climatology indicates that there is more descent in the Southern than in the Northern Hemisphere. Accordingly, isentropic mixing from the SH mixes in older air (with lower N_2O mixing ratios) than the corresponding mixing from the NH. This mostly impacts mixing on the lower isentropes where in the NH the seasonal cycles of carbon dioxide and water vapor are still evident. Some of the scatter in the plots, for example, for the 951105 and 970923 profiles where the slopes on average are pretty close to that of $(N_2O)_{tr}$, is probably caused by the flight-to-flight variability in the measured value of tropospheric N_2O, consistent with published uncertainties in measured N_2O. For the 961211 flight there is apparently not enough low N_2O air required for mixing below 420 K and too much mixing required between 420 and 460 K. This discrepancy, equally evident for both Southern and Northern Hemisphere mixing, could result from variability in the seasonal fit of CO_2 to N_2O as well as the limitation of using average seasonal correlations of N_2O and potential temperature at midlatitudes.

In Figure 7a and 7b we illustrate the values of $(H_2O)_{mbc}$ resulting from mixing Southern and Northern Hemisphere air, respectively, using H_2O-N_2O correlations in Figure 4, along with the same representation of $(H_2O)_{bc}$ from saturation mixing ratios as in Figure 3b. These figures together summarize the degree to which $(H_2O)_{bc}$ is constrained by the analysis using the photochemical model and in situ data. They also illustrate how well the particular representation of $(H_2O)_{bc}$ derived from saturation mixing ratios meets those constraints. For the 951105 and 970923 flights the water vapor profiles or $(H_2O)_{mbc}$ in Figures 7a and 7b are remarkably similar, illustrating the lack of dependence on the details of the mixing. Analyses of these two flights suggest a strong potential for constraining the water vapor boundary condition. On the one hand, the 960213 profile is of limited utility, because the mixing does not improve the agreement between $(CO_2)_{mbc}$ and $(CO_2)_{bc}$, especially for air most recently entering the stratosphere. On the other hand, it is interesting to postulate that the reason for the poor fit for air sampled below the 405 K isentrope, with water vapor values less than 3 ppmv, is that this air was convectively transported into the lower stratosphere, consistent with both the CO_2 and the H_2O mixing ratios. Comparing the results for the 961211 flight in Figures 7a and 7b illustrates a clear difference in the region corresponding to where there is a large amount of midlatitude mixing. While the structure in the water vapor profile that results from using NH mixing is probably not real, it cannot be ruled out a priori and therefore provides uncertainty in $(H_2O)_{bc}$. The 960801 and 960808 flights provide an opportunity to compare the process for two flights temporally

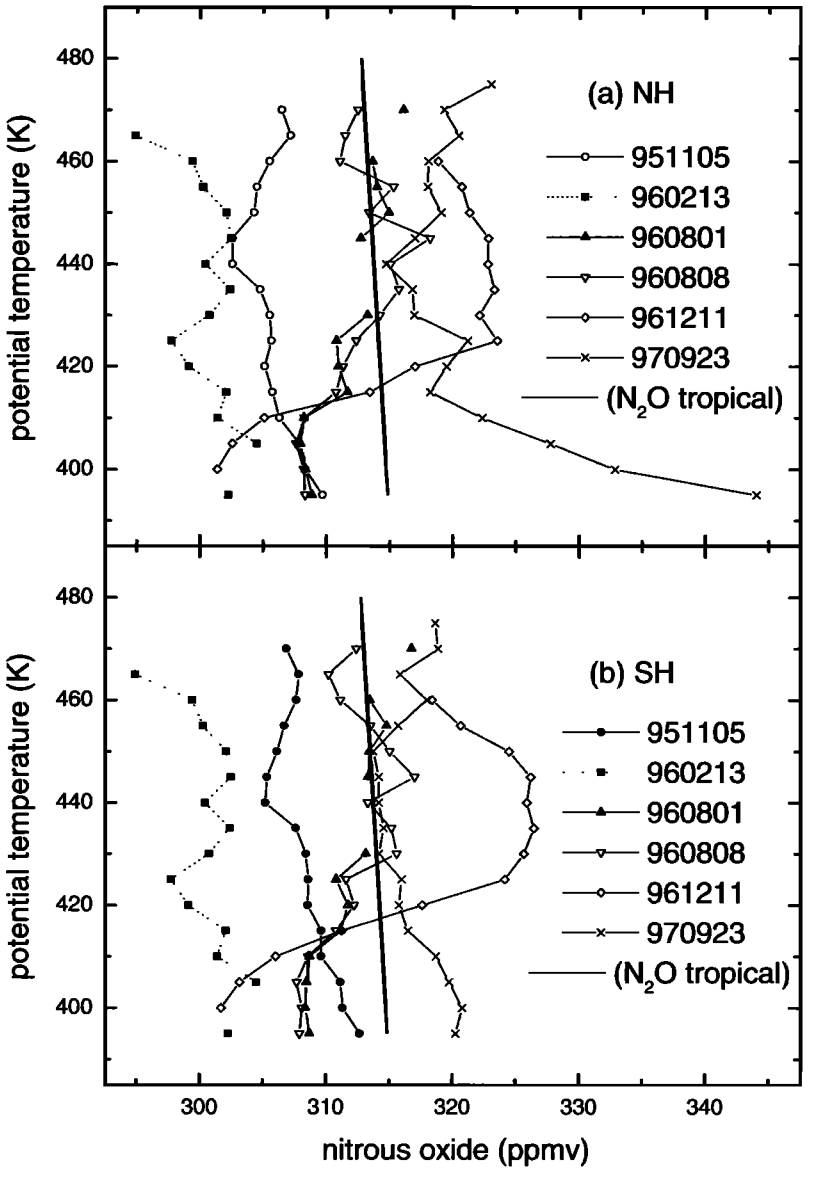

Figure 6. Mixing ratios of N_2O for the 951105, 960213, 960801, 960808, 961211, and 970923 flights derived identically to CO_2 as presented in Figure 5 and plotted versus potential temperature. Presented as well is an N_2O profile derived by assuming a tropospheric value of 315 ppbv and a decay with potential temperature based on a 63-year lifetime and a 0.53K/d ascent rate. Figures 6a and 6b result from using Northern and Southern Hemisphere air, respectively.

close together, analyzed independently, and, as shown in Table 1, that require significantly different amounts of admixed air. The largest difference between the two flights is from data taken below 415 K and could be caused by the natural variability of water vapor entering the tropical stratosphere. Nevertheless, the differences in the 960801 and 960808 plots of $(H_2O)_{mbc}$ provide an example of the uncertainty with which $(H_2O)_{mbc}$ is constrained and indicate the utility and necessity of more than one flight within a season. Additionally, the self- consistency of the 960801, 960808, and 961211 profiles provide further evidence of the promise this analysis shows.

We have demonstrated in Figure 5 the degree to which the change in the measured time series of carbon dioxide (and water vapor in Figure 7) mixing ratios in the lower tropical stratosphere can be attributed to midlatitude mixing. The mixing scenario illustrates the utility of using high-resolution in situ measurements of tracers that exhibit seasonal variability, an extension beyond previously cited studies that investigate annually averaged transport processes. In addition, several studies have used simple numerical models to simulate the propagation and attenuation of the H_2O and CO_2 seasonal signals. These studies typically assume that the amplitude of the seasonal signal at midlatitude is zero, which is not consistent with our observations (Figure 4) or the Stratospheric Aerosol and Gas Experiment (SAGE) II [*McCormick et al.*, 1993] and HALOE [Mote *et al.*, 1995, 1996] water vapor observations.

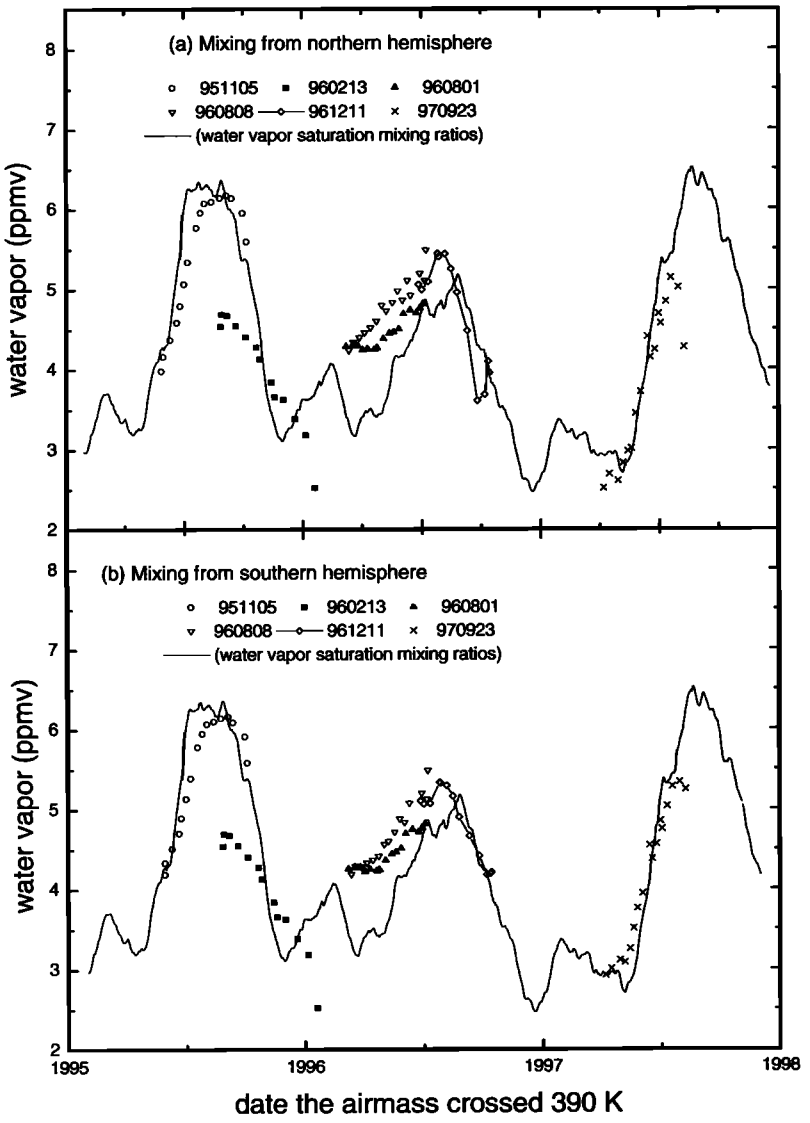

Figure 7. Mixing ratios of H_2O for the 951105, 960213, 960801, 960808, 961211, and 970923 flights derived identically to CO_2 as presented in Figure 5. Included is a plot of $(H_2O)_{bc}$ derived from a 30-day running mean of saturation mixing ratios derived from radiosonde cold-point temperature measurements between 10°S and 10°N, as in Figure 4b. figure 7a and 7b result from using Northern and Southern Hemisphere air, respectively.

6. Uncertainties

In this paper we have developed a technique to quantitatively investigate the relationship between water vapor mixing ratios measured in the stratosphere and a representation of stratospheric entry-level (or boundary condition) mixing ratios. We provide as an example of these boundary condition values saturation mixing ratios derived from tropical tropopause temperatures. It is important to understand what the limits of this kind of investigation are and what needs to be accomplished to constrain $(H_2O)_{bc}$. The process requires accurate high-resolution water vapor measurements and a framework to relate $(H_2O)_m$ and $(H_2O)_{bc}$, which in our analysis is a determination of the time the air has been in the stratosphere, and a treatment of mixing.

Regarding the latter and, similarly, using the photochemistry of CO, *Flocke et al.* [1999] suggest that average ascent rates in the lower tropical stratosphere have an uncertainty of 44% arising from a 30% uncertainty in the OH + CO reaction, a 30% uncertainty in OH, and a 10% uncertainty in measured CO. The agreement in phase between $(CO_2)_{mbc}$ and $(CO_2)_{bc}$ suggests that either the uncertainties are extremely conservative or there is a fortuitous cancellation of errors. Accurate measurements of slightly longer-lived organic molecules without a stratospheric source term would enable a more accurate determination valid to higher potential temperatures and would nicely complement the CO photochemistry. While profiles of molecules fitting these specifications have been used in the analysis of annually averaged isentropic mixing into the lower stratosphere [*Flocke et al.*, 1999], current aircraft instrumentation does not provide adequate signal to noise and response time to allow flight-to-flight analysis. Data sufficient for this purpose could be obtained either by improved experimental techniques or by

the use of aircraft capable of much slower ascent and descent rates than the ER-2.

Because we use CO_2 mixing ratios to identify the amount of midlatitude air mixed into the tropics, uncertainties in the relationship between CO_2 and H_2O mixing ratios on each N_2O isopleth contribute to the uncertainty of the derived water vapor boundary condition. This is not a serious problem when mixing from the SH is used because the N_2O:θ correlation in the Strahan SH climatology constrains the mixing to isopleths with a maximum N_2O value of 285 ppbv. For mixing from the NH, typically only a small fraction of the mixing occurs on isopleths with N_2O mixing ratios greater than 290 ppbv. Uncertainties of 25% in the fit to the midlatitude H_2O data should cause only small errors in the derived values of $(H_2O)_{mbc}$. Nevertheless, comprehensive measurements in the lower stratosphere of the Northern and Southern Hemispheres would be advisable to complement tropical measurements needed to continue this analysis approach for determining $(H_2O)_{bc}$.

We now consider in more detail the uncertainties in our in situ water vapor measurements and in boundary condition water vapor derived from monthly average saturation mixing ratios. We start by looking at how the use of water vapor measurements made by other instruments might affect our results. Direct comparisons of our water vapor instrument with two other *in situ* instruments on the NASA ER-2 have been described in the literature. In 1993, as described by *Weinstock et al.* [1994] and *Hintsa et al.* [1994], our instrument systematically measured 15% higher than the NOAA Lyman-α hygrometer [*Kelly et al.*, 1989]. In 1997, as described by *Hintsa et al.* [1999], our instrument agreed with a near-infrared tunable diode laser spectrometer [*May*, 1998] to better than 5%, with agreement best near ER-2 cruise altitudes at ambient pressures for which the diode laser spectrometer was optimized. Indirect comparisons can also be made with instruments that have produced data sets from which annually averaged entry-level water vapor mixing ratios in air entering the stratosphere can be derived. Such a comparison, tabulated by *Dessler* [1998], implies that the Harvard hygrometer systematically measures 10-25% higher than other (*in situ* and remote) hygrometers. It is beyond the scope of this paper to evaluate these differences in detail, and the above analysis cannot discriminate between different stratospheric water vapor boundary conditions without the adjudication of these discrepancies. Nevertheless, without the successful resolution of this issue, evaluation of the stratospheric water vapor boundary condition will be obscured by instrumental differences.

Because we use saturation mixing ratios derived from tropopause temperatures to establish a representation of $(H_2O)_{bc}$, we next investigate potential errors in $(H_2O)_{bc}$ resulting from using radiosonde data. Radiosonde stations are not distributed homogeneously throughout the tropics. We first investigate any potential bias this might cause by comparing National Meteorological Center (NMC) [*Gelman et al.*, 1994] and United Kingdom Meteorological Office (UKMO) [*Swinbank and O'Neill*, 1994] 100 mbar average temperatures within 10°S and 10°N with average NMC and UKMO temperatures weighted according to the distribution of the radiosonde stations. The monthly average-weighted temperatures, the monthly average temperatures using all the grid points within 10°S and 10°N, and the monthly average radiosonde temperatures are displayed in Figure 8. The UKMO and NMC comparisons show that the weighted

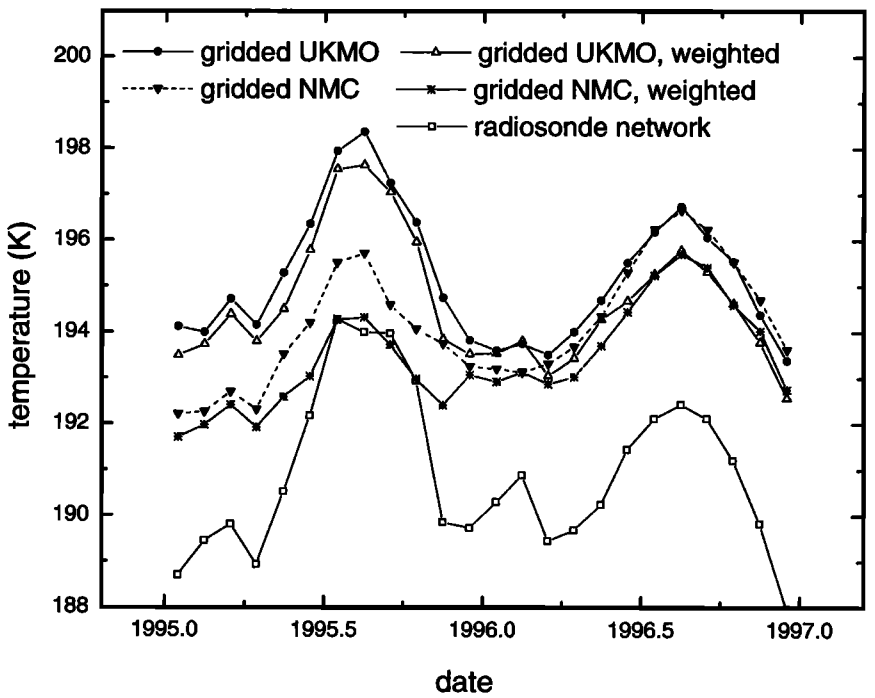

Figure 8. Monthly tropopause temperatures averaged from all radiosonde stations between 10°N and 10°S for 1995 and 1996. Plotted are monthly 100 mbar temperatures averaged using all NMC and UKMO grid points between 10°S and 10°N and monthly 100 mbar temperatures averaged using only NMC and UKMO grid points approximately collocated with tropical radiosonde stations.

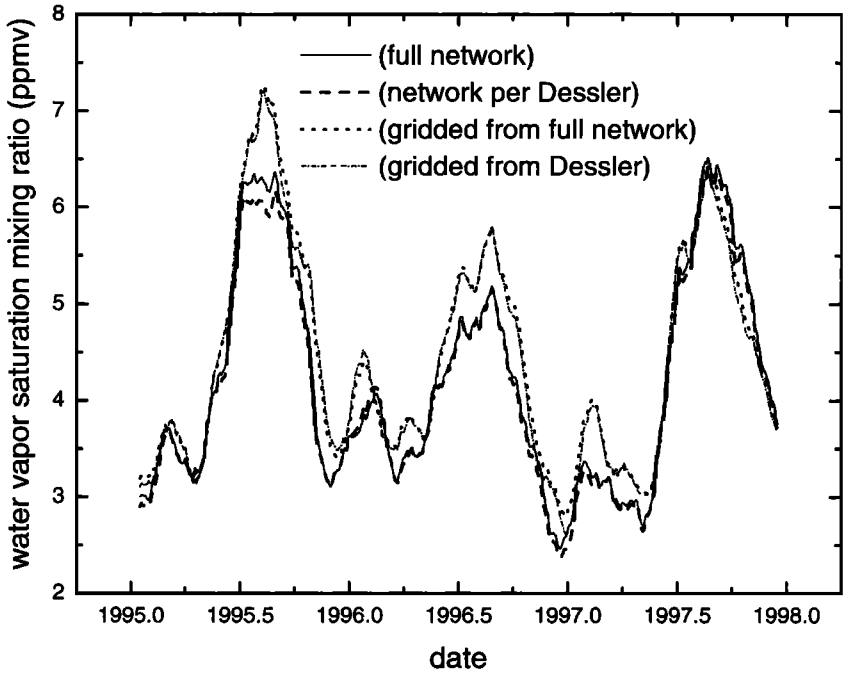

Figure 9. Plots of running mean WVSMRs derived from cold-point temperatures from radiosonde data between 10°S and 10°N. Shown are the average of all WVSMRs (solid line), the mean WVSMR of a grid onto which the individual minimum WVSMRs were interpolated (dotted line), a somewhat reduced number of stations, pruned to match the stations used by Dessler (dashed line), and the mean WVSMR of a grid onto which the individual minimum WVSMRs from the stations used by Dessler were interpolated (dotted-dashed line).

monthly averages have annual average negative biases of about 0.5-0.6 K and 0.7-0.8 K, respectively, relative to the unweighted averages. These biases also exhibit annual and interannual variability, with the bias largest during northern summer.

It is also relevant that NMC and UKMO 100 mbar temperatures shown in Figure 8 exhibit, on average, a 3-4 K warm bias relative to measured radiosonde tropopause temperatures. This bias is consistent with that exhibited in Figure 6 of *Highwood and Hoskins* [1998], which compares a climatology of tropopause temperature from the European Center for Medium-Range Weather Forecasts (ECMWF) with radiosonde data. Figure 8 illustrates that using saturation mixing ratios derived from average NMC or UKMO 100 mbar temperatures would result in a significantly wetter stratosphere (in all seasons) than indicated by the radiosonde temperatures as well as by our observations. Therefore while we believe that the bias caused by the lack of homogeneous radiosonde coverage in the tropics is qualitatively significant, we do not believe that we can use these data to correct for the cold bias on a monthly basis.

Another approach that can be used to evaluate any bias resulting from the distribution of radiosonde stations is to use data from the existing stations to produce a homogeneous grid of WVSMRs that would then provide a daily average value approximating the entire 10°N to 10°S latitudinal band. Interpolation was done using a weighting factor of exp[-(d/s)^2], where d is the distance between a given grid point and a sounding station, and s is a distance scale chosen to be approximately equal to the decorrelation distance calculated for WVSMRs among the various sounding stations. Figure 9 shows the original results from the average of all WVSMRs (solid line), the mean WVSMR of a grid onto which the individual minimum WVSMR were interpolated (dotted line), a somewhat reduced number of stations, pruned to match the stations used by *Dessler* [1998] (dashed line), and the mean WVSMR of a grid onto which the individual minimum WVSMR from the stations used by Dessler were interpolated (dot-dash line). Note however, that even the full sounding set has large gaps, especially in the eastern equatorial Pacific. These plots give a fairly consistent picture that on an annual basis, the bias in calculated mean WVSMR caused by the distribution of radiosonde stations is about -0.3 ± 0.1 ppmv with more of the bias showing up in the summer months.

7. Conclusions

In this manuscript we have described a process that uses simultaneous in situ measurements of water vapor, carbon dioxide, carbon monoxide, and nitrous oxide and a simple photochemical model to investigate the degree to which the seasonal cycle of water vapor entering the stratosphere can be constrained. We have demonstrated that for five out of the six flights into the lower tropical stratosphere $(CO_2)_{mbc}$ matches $(CO_2)_{bc}$ very well when midlatitude mixing is appropriately taken into account. Accordingly, we have "validated" the photochemical ages of the sampled stratospheric air. These ages can be used to calculate average ascent rates in the lower tropical stratosphere that can be compared with those determined using in situ CO_2 data [*Boering et al.*, 1994; *Andrews et al.*, 1999], satellite data, and a radiative transfer model [*Eluszkiewicz et al.*, 1996, 1997; *Rosenlof et al.*, 1997], and a one-dimensional (1-D) advection-diffusion-dilution model, [*Mote et al.*, 1998]. While such a comparison is

beyond the scope of this paper, it is interesting to note that the derived ascent velocities, as calculated from ages presented in Figure 2, are higher in northern summer than in northern winter. This seasonal dependence is inconsistent with our current understanding of the dynamics driving the circulation and with independent estimates of the tropical vertical ascent rates, both of which indicate faster ascent during NH winter when wave-induced drag is most effective. On the one hand, there are assumptions in our calculations that, in principle, could cause an incorrect seasonal signature on the calculated velocities. It is possible that the neglect of midlatitude mixing in the calculation of photochemical age is more significant than expected. Also, the assumption that CO at the 390 K isentrope does not have a seasonal dependence could impose an incorrect seasonality on the calculated stratospheric ages. On the other hand, the phase agreement between $(CO_2)_{mbc}$ and $(CO_2)_{bc}$ provides evidence that the calculated ages are correct. As a result, we are left with a conundrum that hopefully can be resolved with more data.

The agreement between the $(H_2O)_{mbc}$ in Figures 7a and 7b, although from only a limited amount of data, suggests the possibility of constraining the water vapor boundary condition mixing ratio to better than 10%. However, any conclusions we reach, based on the agreement between $(H_2O)_{mbc}$ and $(H_2O)_{bc}$, clearly depend on the accuracy of the in situ water vapor data used in the analysis. Furthermore, there are clear regions, especially between December and May (which includes the season with the lowest water vapor), for which there are no data or the constraint on $(H_2O)_{bc}$ is poor.

During the times when $(H_2O)_{bc}$ is constrained by $(H_2O)_{mbc}$, water vapor saturation mixing ratios derived from tropopause temperatures measured between 10°N and 10°S provide a reasonable boundary condition for water vapor entering the stratosphere. For the 1995 summer period, the saturation mixing ratios calculated from equally spaced grid points (Figure 9) are too high. During the summer of 1996, while there is some disagreement in phase, the water vapor from the grid points agrees better with $(H_2O)_{mbc}$. Accordingly, at this time, neither is there enough data nor is the constraint sufficient to distinguish between $(H_2O)_{bc}$ directly averaged from the radiosonde network or that derived from an average of the interpolated grid. In fact, if the premise that water vapor is controlled by local tropopause temperatures is accepted, then the data are evidence for a difference between 1995 and 1996 regarding the geographic distribution of air entering the stratosphere.

This analysis suggests that it is premature to either accept or reject the "stratospheric-fountain" hypothesis to explain the water vapor budget of the stratosphere. The seasonal coverage and temporal resolution of the data provide the means for a more stringent test of the boundary condition than the annual average examined by *Dessler* [1998]. It also must be said however, that without extending the longitudinal coverage of the radiosonde network in the tropics significantly, it is unclear whether an analysis similar to that presented here could be used to identify where in the tropics air is entering the stratosphere, and where it is not. Because we are attempting to determine the seasonal cycle of water vapor entering the stratosphere, our determination of the seasonal cycle of water vapor will not necessarily yield the same value of $(H_2O)_e$ as *Dessler* [1998] or *Hurst et al.* [1999]. Our analysis attempts to derive water vapor mixing ratios entering the stratosphere prior to the admixture of midlatitude air, while previous determinations all result from analyses after this mixing has occurred. Any difference in the value of $(H_2O)_e$ derived from these two determinations cannot be ruled out a priori. Our analysis also shows that for CO_2 (and by extension water vapor), for five out of six flights, the differences between profile values measured above the tropopause and boundary-condition mixing ratios can be explained by the entrainment of midlatitude stratospheric air in amounts consistent with previous studies.

With the above caveats, this paper provides evidence that water vapor entering the tropical lower stratosphere as measured by the Harvard University photofragment fluorescence hygrometer is consistent with saturation mixing ratios derived from tropical tropopause temperatures. These results are consistent with current theories [*Jensen et al.*, 1996a, 1996b] and recent observations that point to the presence of thin (subvisible) cirrus clouds near the tropical tropopause [*Wang et al.*, 1996] as an indication of dehydration during large-scale slow ascent with the concomitant settling out of large particles. Additionally, by demonstrating that tropical tropopause temperatures are consistent with stratospheric water vapor, we provide a focal point where models can investigate potential changes in stratospheric water vapor based on the tropopause response to anthropogenically induced changes in the atmosphere. However, the analysis cannot rule out the possibility that the flux through the tropopause exhibits an annually dependent longitudinal (or other geographical) dependence, and it does not uniquely identify a specific dehydration mechanism. While the overall apparent agreement would tend to support dehydration during slow ascent across the tropopause rather than convective transport across it, we cannot rule out the convective scheme proposed by *Sherwood and Dessler* [2001]. Uncertainties in radiosonde temperatures and the apparent inadequacy of radiosonde coverage in the tropics suggest that the analysis used here is not likely to provide an unambiguous answer to the stratospheric fountain question. While improving the distribution of radiosondes in the tropics would help, a more comprehensive approach is needed.

Understanding the details of stratosphere-troposphere exchange, similar to understanding problems such as stratospheric ozone depletion and global climate change, can benefit from two investigative strategies. Time series measurements, limited by available measurement precision and accuracy, are used to evaluate changes or trends in data sets. Searches are made for correlations with variables thought to be the potential cause of these observed changes or trends. At the same time, measurement programs are carried out that are designed to test specific mechanistic hypotheses. The STEP program in 1984 and 1987 was the last such program designed to specifically investigate STE. Recently, trends in stratospheric water vapor have been detected by satellite measurements [*Evans et al.*, 1998] and by *in situ* frost point measurements at midlatitudes [*Oltmans and Hoffman*, 1995; *Oltmans et al.*, 2000]. On the other hand, the analysis of the water vapor budget of the stratosphere by *Hurst et al.* [1999] does not support an increase in stratospheric water vapor between 1993 and 1997, nor has a cause of a potential increase in stratospheric water vapor been identified. At this time, when stratospheric ozone depletion and global climate change have been directly linked to changes in the water vapor budget of the stratosphere, it is imperative that we evaluate existing data and delineate sets of measurements

needed to test prevailing theories of troposphere-to-stratosphere transport.

Acknowledgments. We thank Paul Wennberg for initially suggesting the use of CO as a photochemical clock. We thank Andrew Dessler for providing averages of the radiosonde data, and along with Paul Newman for facilitating access to radiosonde, WMO, and UKMO temperature data on the NASA Goddard computer network. This research was funded in part by NASA grants NCCC-913 and NCC2-694 to Harvard University. Work at the Jet Propulsion Laboratory, California Institute of Technology, was done under contract to NASA.

References

Abbas M. M., et al., Seasonal variations of water vapor in the lower stratosphere inferred from ATMOS/ATLAS-3 measurements of H_2O and CH_4, *Geophys. Res. Lett., 23*, 2401-2404, 1996.

Andrews, A. E. et al., Empirical age spectra for the lower tropical stratosphere from in situ observations of CO_2: Implications for stratospheric transport, *J. Geophys. Res., 104*, 26,581-26,595, 1999.

Avallone, L. M., and M. J. Prather, Photochemical evolution of ozone in the lower tropical stratosphere, *J. Geophys. Res., 101*, 1457-1461, 1996.

Boering, K. A., B. C. Daube, S. C. Wofsy, M. Loewenstein, J. R. Podolske, and E. R. Keim, Tracer-tracer relationships and lower stratospheric dynamics: CO_2 and N_2O correlations during SPADE, *Geophys. Res. Lett., 21*, 2567-2570, 1994.

Boering, K. A., et al., Measurements of stratospheric carbon dioxide and water vapor at northern midlatitudes: Implications for troposphere-to-stratosphere transport, *Geophys. Res. Lett., 22*, 2737-2740, 1995.

Boering, K. A., et al., Stratospheric mean ages and transport rates from observations of carbon dioxide and nitrous oxide, *Science, 274*, 1340-1343, 1996.

Brewer, A. W., Evidence for a world circulation provided by measurements of He and H_2O in the stratosphere, *Q. J. R. Soc., 75*, 351-363, 1949.

Conway, T. J., et al., Evidence for interannual variability of the carbon cycle from the National Oceanic and Atmospheric Administration/Climate Monitoring and Diagnostics Laboratory global air sampling network, *J. Geophys. Res., 99*, 22,831-22,855, 1994.

Danielsen, E. F., A dehydration mechanism for the stratosphere, *Geophys. Res. Lett., 9*, 605-608, 1982.

Danielsen, E. F., In situ evidence of rapid vertical irreversible transport of lower tropospheric air into the lower tropical stratosphere by convective cloud turrets and by larger-scale upwelling in tropical cyclones, *J. Geophys. Res., 98*, 8665-8681, 1993.

DeMore, W. B., et al., Chemical kinetics and photochemical data for use in stratospheric modeling, *Evaluation 12, JPL Publ., 97-4*, Jet Propul. Lab., Pasadena, CA, 1997.

Dessler, A. E., A reexamination of the "stratospheric fountain" hypothesis, *Geophys. Res. Lett., 25*, 4165-4168, 1998.

Eluszkiewicz, J., et al., Residual circulation in the stratosphere and lower mesosphere as diagnosed from microwave limb sounder data, *J. Atmos. Sci., 53*, 217-240, 1996.

Eluszkiewicz, J., et al., Sensitivity of the residual circulation diagnosed from the *UARS* data to the uncertainties in the input fields and to the inclusion of aerosols, *J. Atmos. Sci., 54*, 1739-1757, 1997.

Evans, S. J., et al., Trends in stratospheric humidity and the sensitivity of ozone to these trends, *J. Geophys. Res., 103*, 8715-8725, 1998.

Flocke, F., et al., An examination of chemistry and transport processes in the tropical lower stratosphere using observations of long-lived and short-lived compounds obtained during STRAT and POLARIS, *J. Geophys. Res., 104*, 26,625-26,642,1999.

Gelman, M. E., A. J. Miller, R. M. Nagatani, and C. S. Long, Use of UARS data in the NOAA stratospheric monitoring program, *Adv. Space Res., 14*(9), 21-31, 1994.

Haynes, P. H., et al., On the "downward control" of extratropical diabatic circulations by eddy-induced mean zonal forces, *J. Atmos. Sci., 48*, 641-678, 1991.

Herman, R. L., et al., Tropical entrainment time scales inferred from stratospheric N_2O and CH_4 observations, *Geophys. Res. Lett., 25*, 2781-2884, 1998.

Herman, R. L., et al., Measurements of CO in the upper troposphere and lower stratosphere, *Chem. Global Change Sci., 1*, 173-183, 1999.

Highwood, E. J., and B. J. Hoskins, The tropical tropopause, *Q. J. R. Meteorol. Soc., 124*, 1579-1604, 1998.

Hintsa, E. J., E. M. Weinstock, A. E. Dessler, J. G. Anderson, M. Loewenstein, and J. R. Podolske, SPADE H_2O measurements and the seasonal cycle of water vapor, *Geophys. Res. Lett., 21*, 2559-2562, 1994.

Hintsa, E. J., E. M. Weinstock, J. G. Anderson, and R. D. May, On the accuracy of in situ water vapor measurements in the troposphere and lower stratosphere with the Harvard Lyman-α hygrometer, *J. Geophys. Res., 104*, 8183-8189,1999.

Holton, J. R., P. H. Haynes, M. E. McIntyre, A. R. Douglass, R. B. Rood, and L. Pfister, Stratosphere-troposphere exchange, *Rev. Geophys. Res., 33*, 403-439, 1995.

Hurst, D. F., et al., Closure of the total hydrogen budget of the northern extratropical lower stratosphere, *J. Geophys. Res., 104*, 8191-8190, 1999.

Jackson, D. R., S. J. Driscoll, E. J. Highwood, J. E. Harries, and J. M. Russell III, Troposphere to stratosphere transport at low latitudes as studied using HALOE observations of water vapour 1992-1997, *Q. J. R.. Meteorol. Soc., 124*, 169-192, 1998.

Jensen, E. J., O. B. Toon, L. Pfister, and H. B. Selkirk, Dehydration of the upper troposphere and lower stratosphere by subvisible cirrus clouds near the tropical tropopause, *Geophys. Res. Lett., 23*, 825-828, 1996a.

Jensen, E. J., O. B. Toon, H. B. Selkirk, J. D. Spinhirne, and M. R. Schoeberl, On the formation and persistence of subvisible cirrus clouds near the tropical tropopause, *J. Geophys. Res., 101*, 21,361-21,375, 1996b.

Kelly, K. K., et al., Dehydration in the lower Antarctic stratosphere during late winter and early spring, 1987, *J. Geophys. Res., 94*, 11,317-11,357, 1989.

Kirk-Davidoff, D. B., E. J. Hintsa, J. G. Anderson, and D. W. Keith, The effect of climate change on ozone depletion through changes in stratospheric water vapor, *Nature, 402*, 399-401,1999.

Kley, D., E. J. Stone, W. R. Henderson, J. W. Drummond, W. J. Harrop, A. L. Schmeltekopf, T. L. Thompson, and R. H. Winkler, In situ measurements of the mixing ratio of water vapor in the stratosphere, *J. Atmos. Sci., 36*, 2513-2524, 1979.

Le Texier, H., S. Solomon, and R. R. Garcia, The role of molecular hydrogen and methane oxidation in the water vapour budget of the stratosphere, *Q. J. R. Meteorol. Soc., 114*, 281-295, 1988.

Luers, J. K., and R. E. Eskridge, Use of radiosonde temperature data in climate studies, *J. Clim., 11*, 1002-1019, 1998.

May, R. D., Open-path, near-infrared tunable diode laser spectrometer for atmospheric measurements of H_2O, *J. Geophys. Res., 103*, 19,161-19,172, 1998.

McCormick, M. P., et al., Annual variations of water vapor in the stratosphere and upper troposphere observed by the Stratospheric Aerosol and Gas Experiment II, *J. Geophys. Res., 98*, 4867-4874, 1993.

Michelsen, H. A., F. W. Irion, G. L. Manney, G. C. Toon, and M. R. Gunson, Features and trends in Atmospheric Trace Molecule Spectroscopy (ATMOS) Version 3 stratospheric water vapor and methane measurements, *J. Geophys. Res., 105*, 22,713-22,724, 2000.

Minschwaner, K., et al., The bulk properties of isentropic mixing into the tropics in the lower stratosphere, *J. Geophys. Res., 101*, 9433-9439, 1996.

Mote, P. W., et al., Seasonal variations of water vapor in the tropical lower stratosphere, *Geophys. Res. Lett., 22*, 1093-1096, 1995.

Mote, P. W., et al., An atmospheric tape recorder: The imprint of tropical tropopause temperatures on stratospheric water vapor, *J. Geophys. Res., 101*, 3989-4006, 1996.

Mote, P. W., et al., Vertical velocity, vertical diffusion, and dilution by midlatitude air in the tropical lower stratosphere, *103*, 8651-8666, 1998.

Murphy, D. M., et al., Reactive nitrogen and its correlation with ozone in the lower stratosphere and upper troposphere, *J.Geophys. Res., 98*, 8751-8773, 1993.

Neu, J. L., and R. A. Plumb, Age of air in a "leaky pipe" model of

stratospheric transport, *J. Geophys. Res., 104*, 19,243-19,256, 1999.

Newell, R. E., and S. Gould-Stewart, A stratospheric fountain?, *J. Atmos. Sci., 38*, 2789-2796, 1981.

Oltmans, S. J., and D. J. Hoffman, Increase in lower-stratospheric water vapor at a mid-latitude Northern Hemisphere site from 1981 to 1984, *Nature, 374*, 146-149, 1995.

Oltmans, S. J., H. Voemel, D. J. Hoffman, K. H. Rosenlof, and D. Kley, The increase in stratospheric water vapor from balloonborne, frostpoint hygrometer measurements at Washington, D. C., and Boulder, Colorado, *Geophys. Res. Lett., 27*, 3453-3456, 2000.

Plumb, R. A., A "tropical pipe" model of stratospheric transport, *J. Geophys. Res.,101*, 3957-3972, 1996.

Podolske, J. R., and M. Loewenstein, Airborne tunable diode laser spectrometer for trace gas measurements in the lower stratosphere, *Appl. Opt., 32*, 5324-5333, 1993.

Reed, R. J., and C. L. Vleck, The annual temperature variation in the lower tropical stratosphere, *J. Atmos. Sci., 26*, 163-167, 1969.

Reid, G. C., and K. S. Gage, On the annual variation in height of the tropical tropopause, *J. Atmos. Sci., 38*, 1928-1938, 1981.

Reid, G. C., and K. S. Gage, The tropical tropopause over the western Pacific: Wave driving, convection, and the annual cycle, *J. Geophys. Res., 101*, 21,233-21,241, 1996.

Rosenlof, K. H., et al., Hemispheric asymmetries in water vapor and inferences about transport in the lower stratosphere, *J. Geophys. Res., 102*, 13,213-13,234, 1997.

Russell, P. B., L. Pfister, and H. B. Selkirk, The tropical experiment of the stratosphere-troposphere exchange project (STEP): Science objectives, operations, and summary findings, *J. Geophys. Res., 98*, 8563-8589, 1993.

Scott, S. G., T. P. Bui, K. R. Chan, and S. W. Bowen, The meteorological measurement system on the NASA ER-2 aircraft, *J. Atmos. Oceanic Technol., 7*, 525-540, 1990.

Seidel, D. J., R. J. Ross, and J. K. Angell, Climatological Characteristic of the tropical tropopause as revealed by radiosondes, *J. Geophys. Res., 106*, 7857-7878, 2001.

Sherwood, S. C., and A. E. Dessler, On the control of stratospheric humidity, *Geophys. Res. Lett.*, 27, 2513-2516, 2000.

Sherwood, S. C., and A. E. Dessler, A model for transport across the tropical tropopause, *J. Atmos. Sci., 58*, 765-779, 2001.

Strahan, S. E., M. Loewenstein, and J. R. Podolske, Climatology and small-scale structure of lower stratospheric N_2O based on in situ observations, *J. Geophys. Res., 104*, 2195-2208, 1999.

Swinbank, R., and A. O'Neill, A stratosphere-troposphere data assimilation system, *Mon. Weather Rev., 122*, 686-702, 1994.

Volk, C. M., et al., Quantifying transport between the tropical and mid-latitude lower stratosphere, *Science, 272*, 1763-1768, 1996.

Voemel, H., and S. J. Oltmans, Comment on "A reexamination of the 'stratospheric fountain' hypothesis," *Geophys. Res. Lett., 26*, 2737-2738, 1999.

Wang, P.-H., et al., A 6-year cloud climatology occurrence frequency from SAGE II observations (1985-1990), *J. Geophys. Res., 101*, 29,407-29,429, 1996.

Webster, C. R., et al., Aircraft (ER-2) laser infrared absorption spectrometer (ALIAS) for in situ stratospheric measurements of HCl, N_2O, CH_4, NO_2, and HNO_3, *Appl. Opt., 33*, 454-472, 1994.

Wennberg, P. O., T. F. Hanisco, R. C. Cohen, R. M. Stimpfle, L. B. Lapson, and J. G. Anderson, In situ measurements of OH and HO_2 in the stratosphere, *J Atmos. Sci., 52*, 3413-3420, 1995.

Wennberg, P. O., et al., Hydrogen radicals, nitrogen radicals, and the production of O_3 in the upper troposphere, *Science, 279*, 49-53, 1998.

Weinstock, E. M., E. J. Hintsa, A. E. Dessler, J. F. Oliver, N. L. Hazen, J. N. Demusz, N. T. Allen, L. B. Lapson, and J. G. Anderson, A new fast response photofragment fluorescence hygrometer for use on the ER-2 and Perseus remotely piloted aircraft, *Rev. Sci. Instrum., 65*, 3544-3554, 1994.

Weinstock, E. M., E. J. Hintsa, A. E. Dessler, and J. G. Anderson, Measurements of water vapor in the tropical lower stratosphere during the CEPEX campaign: Results and interpretation, *Geophys. Res. Lett., 22*, 3231-3234, 1995.

J. G. Anderson, D. B. Kirk-Davidoff, and E. M. Weinstock, Department of Chemistry and Chemical Biology, Harvard University, 12 Oxford St., Cambridge, MA 02138, USA. (anderson@huarp.harvard.edu; davidoff@huarp.harvard.edu; elliot@huarp.harvard.edu)

T. P.Bui, Ames Research Center, NASA, Moffett Field, CA 94035, USA.

R. L. Herman and C. R. Webster, Jet Propulstion Laboratory, California Institue of Technology, Pasadena, CA 91109, USA.

E. J. Hintsa, Woods Hole Oceanographic Institution, Woods Hole, MA 02543, USA.

A. E. Andrews, NASA Goddard Space Flight Center, Greenbelt, MD 20771, USA.

(Received October 16, 2000; revised March 16, 2001; accepted March 22, 2001.)